

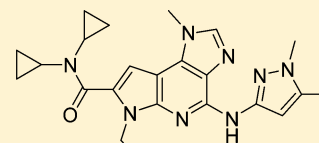
# Discovery of a Highly Selective JAK2 Inhibitor, BMS-911543, for the Treatment of Myeloproliferative Neoplasms

Honghe Wan, Gretchen M. Schroeder, Amy C. Hart, Jennifer Inghrim,<sup>†</sup> James Grebinski,<sup>‡</sup> John S. Tokarski, Matthew V. Lorenzi,<sup>§</sup> Dan You, Theresa Mcdevitt,<sup>§</sup> Becky Penhallow, Ragini Vuppugalla, Yueping Zhang, Xiaomei Gu, Ramaswamy Iyer, Louis J. Lombardo, George L. Trainor,<sup>||</sup> Stefan Ruepp, Jonathan Lippy, Yuval Blat,<sup>⊥</sup> John S. Sack, Javed A. Khan, Kevin Stefanski, Bogdan Slecza, Arvind Mathur, Jung-Hui Sun, Michael K. Wong, Dauh-Rung Wu, Peng Li, Anuradha Gupta,<sup>#</sup> P. N. Arunachalam,<sup>#</sup> Bala Pragalathan,<sup>#</sup> Sankara Narayanan,<sup>#</sup> Nanjundaswamy K.C.,<sup>#</sup> Prakasam Kuppusamy,<sup>#</sup> and Ashok V. Purandare\*

Bristol-Myers Squibb R&D, US Route 206 and Province Line Road, Princeton, New Jersey 08543-4000, United States

## Supporting Information

**ABSTRACT:** JAK2 kinase inhibitors are a promising new class of agents for the treatment of myeloproliferative neoplasms and have potential for the treatment of other diseases possessing a deregulated JAK2-STAT pathway. X-ray structure and ADME guided refinement of C-4 heterocycles to address metabolic liability present in dialkylthiazole **1** led to the discovery of a clinical candidate, BMS-911543 (**11**), with excellent kinome selectivity, *in vivo* PD activity, and safety profile.



**11 (BMS-911543)**  
JAK2 IC<sub>50</sub> = 1.1 nM  
JAK1 / JAK3 / Tyk2 IC<sub>50</sub> (nM) = 360 / 75 / 66  
SET-2 IC<sub>50</sub> = 60 nM

**KEYWORDS:** JAK2, selective inhibitor, myeloproliferative neoplasm, structure-guided design, BMS-911543

Myeloproliferative neoplasms (MPNs) are a subset of myeloid malignancies that are characterized by the expansion of a hematopoietic progenitor stem cell. MPNs encompass polycythemia vera (PV), essential thrombocytopenia (ET), and primary myelofibrosis (PMF).<sup>1</sup> In the majority of cases, this cluster of diseases has been shown to be associated with the somatic mutation JAK2-V617F that constitutively activates the Janus kinase 2 (JAK2) enzyme, a member of the JAK family of nonreceptor tyrosine kinases.<sup>2</sup> In MPNs the acquisition of the JAK2-V617F and other JAK2-STAT pathway mutations result in cytokine-independent activation of the pathway and the uncontrolled growth of hematopoietic cells with erythrocytes, platelets, and granulocyte/monocytes being the predominant lineages expanded in ET, PV, and PMF, respectively.<sup>3</sup> The uncontrolled growth of these cell lineages in MPNs results in severe patient complications including splenomegaly, hemorrhage, thrombosis, bone marrow fibrosis, and transformation to acute myeloid leukemia. The overall survival rate for patients afflicted with advanced myelofibrosis is estimated to be 3–5 years.<sup>4</sup>

The causal role of JAK2 in MPNs is supported by significant genetic and pharmacological data. Transgenic reconstitution of JAK2 mutations into rodent bone marrow stem cells results in a phenotype mirroring the main features of human MPNs including splenomegaly, bone marrow fibrosis, and elevated levels of certain hematopoietic lineages (e.g., erythrocytes, leukocytes).<sup>5</sup> Administration of small molecule JAK2 kinase inhibitors reverses the pathophysiological features of the

transgenic phenotype.<sup>6</sup> Moreover, clinical testing of two small molecule JAK2 inhibitors (e.g., ruxolitinib, fedratinib, pacritinib) showed effects on splenomegaly and normalization of blood counts (Figure 1).<sup>7–9</sup> Based upon the late stage clinical efficacy and tolerability profile, ruxolitinib was approved to treat myelofibrosis (MF). Several other JAK2 inhibitors with varying degrees of JAK family as well as overall kinome selectivity profiles are in mid to late-stage clinical trials for MF.<sup>10</sup> However, it is important to note that most of these compounds also inhibit other JAK family members that could be associated with immunosuppression, an undesired side effect for this indication. Additionally, other off-target kinome activities (e.g., FLT3) could further compromise the anticipated high safety window needed for long-term treatment in MPNs.

We have recently disclosed the identification of a potent and highly selective JAK2 inhibitor **1**.<sup>11</sup> X-ray crystallographic studies of **1** bound to the JAK2 kinase domain indicated that it engages the Tyr931 residue through hydrogen bonding with the thiazole nitrogen atom. In addition, unfavorable interactions of the 4,5-dimethylthiazole fragment with nonconserved residues in the extended hinge region of other JAK family members provided high selectivity. Further ADME profiling indicated that **1** was rapidly metabolized across species and was

Received: June 9, 2015

Accepted: July 12, 2015

Published: July 12, 2015

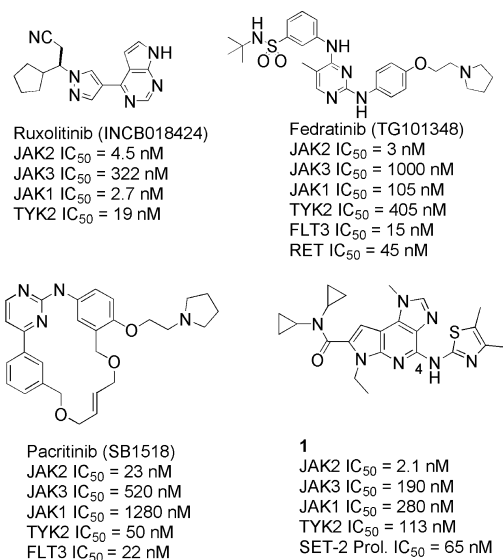


Figure 1. JAK2 inhibitors.

susceptible to generation of reactive metabolites (*vide infra*), which prevented its further progression. Herein we report ADMET and structure-guided optimization of heterocycles at the C-4 position of the imidazopyrrolopyridine core leading to the discovery of a highly selective JAK2 inhibitor, BMS-911543 (11), as a clinical candidate for the treatment of MPNs. Earlier we have reported biological characterization of BMS-911543.<sup>12</sup>

*In vitro* biotransformation studies with compound 1 using human liver microsomes revealed the formation of a thiourea metabolite in significant amounts (15%). This metabolic process presumably involves cytochrome P450-mediated oxidation of the thiazole ring to an epoxide and subsequent opening to form a diol intermediate. Decomposition of the diol intermediate leads directly to a thiourea and diketone species (Figure 2). Thioureas have the potential to form an active metabolite *in vivo*, which could disrupt thyroid function and could also have adverse effects in lung, liver, and bone marrow.<sup>13</sup>

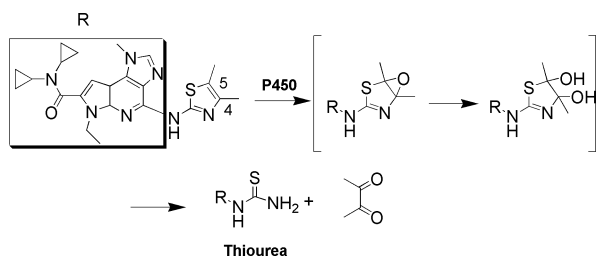
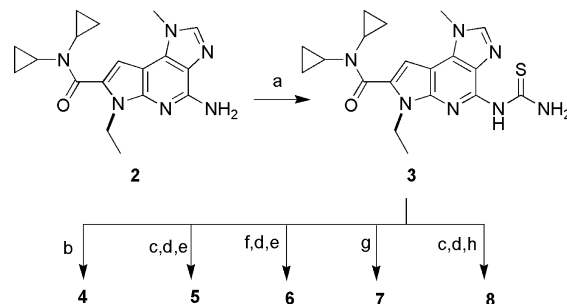


Figure 2. Metabolism of 1.

Literature reports indicated that the introduction of either electron withdrawing groups on the thiazole or increasing sterics may reduce initial complexation with CYP enzymes, which could suppress oxidative ring opening.<sup>13,14</sup> Accordingly, analogues 4–8 were prepared using the approach outlined in Scheme 1, starting from aminopyridine 2.<sup>15,16</sup>

As anticipated, adding substitution on the 4-methyl group (4) maintained the JAK family selectivity profile of the parent compound (Table 1). However, this change still resulted in formation of thiourea in significant amounts in *in vitro* biotransformation studies. Introduction of electron withdraw-

Scheme 1<sup>a</sup>

<sup>a</sup>Reagents and conditions: (a) benzoylthiocyanate, acetone; then 1 N NaOH, ethanol, 60 °C, 72%; (b) 3-bromopentan-2-one, 60 °C, 44%; (c) methyl 2-bromo-3-oxobutanoate, ethanol, 65 °C, 84%; (d) 1 N NaOH, methanol, 65 °C, 93%; (e) methylamine, HATU, 2,6-lutidine, DMF, 75%; (f) methyl 3-bromo-2-oxobutanoate, ethanol, 65 °C, 70%; (g) 1-bromo-1-(methylsulfonyl)propan-2-one ethanol, 65 °C, 62%; (h), 1,1-dioxo-1-thiomorpholine, HATU, 2,6-lutidine, DMF, 62%.

Table 1. Biotransformation and Thiazole Substitution SAR<sup>a,b,c</sup>

Cmpd	R	%Thiourea observed <sup>c</sup>	JAK2 (IC <sub>50</sub> , nM) <sup>a,b</sup>	JAK1 (IC <sub>50</sub> , nM) <sup>a,b</sup>	JAK3 (IC <sub>50</sub> , nM) <sup>a,b</sup>	SET-2 (IC <sub>50</sub> , nM) <sup>a,b</sup>
1		13	2.1	190	280	65
4		23	1.4	250	460	92
5		MS <sup>d</sup>	0.9	19	19	120
6		MS <sup>d</sup>	3.1	22	49	100
7		MS <sup>d</sup>	1.4	40	52	51
8		ND <sup>e</sup>	0.7	48	31	330

<sup>a</sup>Assay protocols are provided in the Supporting Information. <sup>b</sup>Assay results are the average of at least two replicates. <sup>c</sup>Percent thiourea determined in human liver microsomes. <sup>d</sup>Only trace levels detected by mass spectrometry. <sup>e</sup>No data was generated.

ing groups led to identification of potent JAK2 inhibitors (compounds 5–7), which were significantly less susceptible to generation of the thiourea metabolite. However, such substitutions caused considerable erosion of selectivity versus other JAK family kinases. With respect to the selectivity of the amide-containing thiazoles, differences in the JAK family members around JAK2 Gln 853 may provide a rationale for the loss in selectivity observed. The smaller serine present in JAK3 would likely be able to accommodate the larger polar amide-containing analogues. However, the arginine present in JAK1 could be positioned such that a favorable hydrogen bond to the amide at the 4- or 5-position on the thiazole may also contribute to loss of selectivity (Figure 3 for JAK1 model with compound 6). Further steric bulk on the amide (8) failed to

improve JAK family selectivity (compared to **1**) and reduced cellular potency.

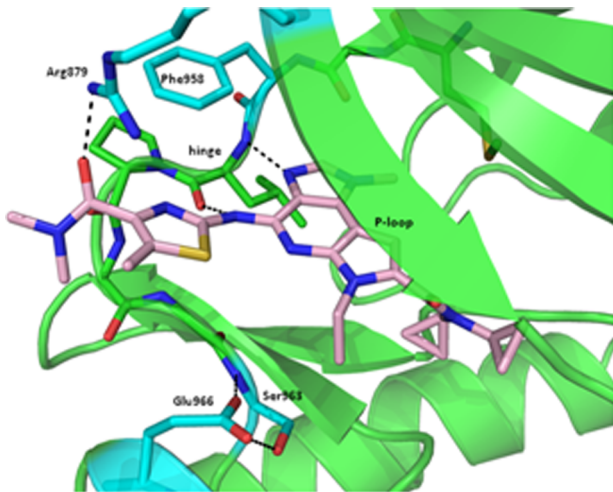
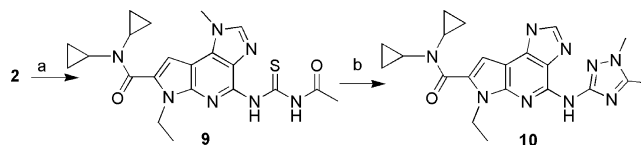


**Figure 3.** Model of **6** bound to the kinase catalytic domain of JAK1. The carbons of **6** are colored in pink, and the carbons for JAK1 are colored in green except for the residues near the C-4 group, which differ in the JAK family (carbons are colored cyan). Oxygen atoms are colored red, nitrogens blue, and sulfurs yellow. Hydrogen bonds are indicated with dashed lines.

We next turned our attention to explore other closely related five-membered isosteric dialkylthiazole ring isosteres that would dispose alkyl groups in the extended hinge region similar to **1** (Table 2). Accordingly, triazole analogue **10** was prepared (Scheme 2).<sup>17</sup>

Triazole **10** displayed modest JAK2 potency and high JAK family selectivity. We postulated the loss of potency may be due to a disfavored interaction of the triazole ring nitrogen with the pyridyl nitrogen forcing the rings to adopt a less planar conformation than compound **1**. Removal of a nitrogen from

**Scheme 2.**<sup>a</sup>



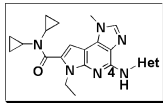
<sup>a</sup>Reagents and conditions: (a) acetyl isocyanate, acetone, 35 °C, 44%; (b) methyl hydrazine, AcOH, 80 °C, 31%.

the triazole ring re-established the planarity (*vide infra*) and led to the discovery of 1,5-dimethyl pyrazole analogue **11**. Compound **11**, henceforth referred to as BMS-911543, displayed an IC<sub>50</sub> of 1.1 nM against JAK2 and was approximately 350-, 75-, and 65-fold selective vs JAK1, JAK3, and TYK2, respectively. Assessment of dissociation constants of BMS-911543 for JAK1, JAK2, and JAK3 indicated greater selectivity with K<sub>i</sub> values of 110, 0.48, and 360 nM, respectively. BMS-911543 was also evaluated in the KinomeScan (formerly Ambit) panel (consisting of 451 kinases) as well as the internal kinase panel to assess overall kinome selectivity. It displayed a high level of selectivity across the kinome (see Supporting Information for complete data set).<sup>18</sup>

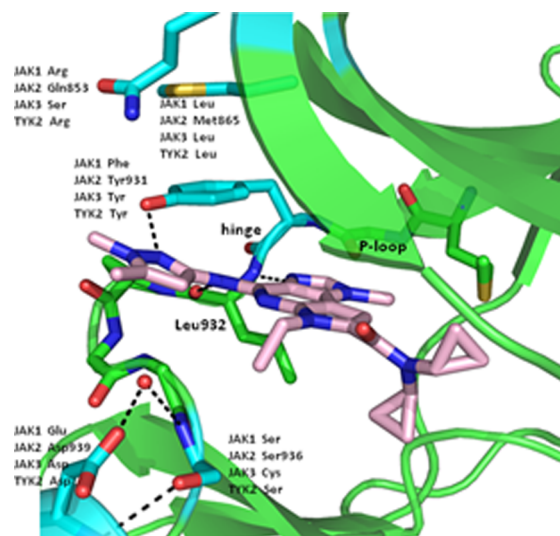
The X-ray structure of BMS-911543 bound to the JAK2 kinase domain displayed a similar binding mode as **1**. One of the nitrogens of the pyrazole ring formed a hydrogen bond with Tyr931 while maintaining coplanarity with the pyrrolopyridine scaffold. The 1,5-dimethyl pyrazole occupied the extended hinge region where key residue differences such as JAK2-Gln853, JAK3-Ser826, JAK1-Arg868, and TYK2-Arg901 resulted in high selectivity within the JAK family (see Figure 4 for location of other nonconserved residues that may affect selectivity).<sup>19</sup>

As expected the introduction of bulkier substitution on the pyrazole nitrogen resulted in further enhancement of selectivity within the JAK family (>140-fold) as observed for the analogue **12** while retaining the positive attributes found in BMS-911543.

**Table 2.** C-4 Heterocycle SAR<sup>a,b</sup>

Cmpd	R					
		JAK2 (IC <sub>50</sub> , nM) <sup>a,b</sup>	JAK1 (IC <sub>50</sub> , nM) <sup>a,b</sup>	JAK3 (IC <sub>50</sub> , nM) <sup>a,b</sup>	TYK2 (IC <sub>50</sub> , nM) <sup>a,b</sup>	SET-2 (IC <sub>50</sub> , nM) <sup>a,b</sup>
<b>1</b>		2.1	190	280	280	65
<b>10</b>		33	6000	3800	ND	1300
<b>11</b>		1.1	75	360	66	60
<b>12</b>		1.5	330	210	220	55
<b>13</b>		230	540	5000	2300	>2000
<b>14</b>		1.2	16	87	1.9	53

<sup>a</sup>Assay protocols are provided in the Supporting Information. <sup>b</sup>Assay results are the average of at least two replicates.

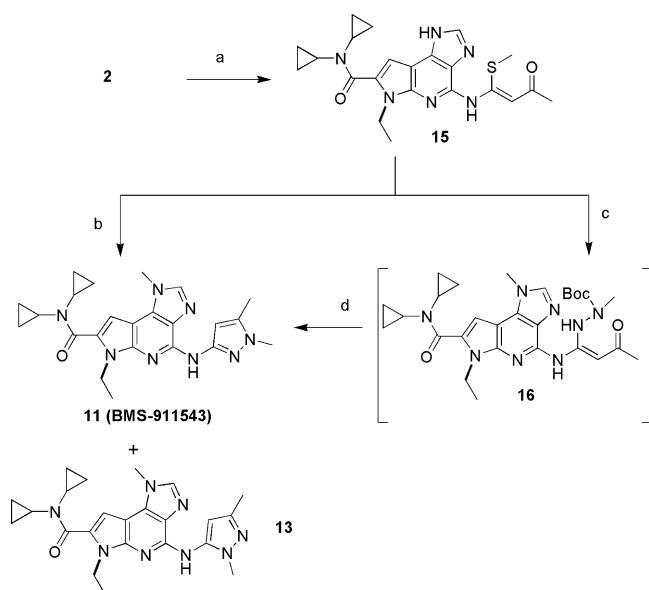


**Figure 4.** Crystal structure of BMS-911543 bound to the kinase catalytic domain of JAK2. The carbons of BMS-911543 are colored in pink and the carbons for JAK2 are colored in green except for the residues near the C-4 group, which differ in the JAK family (carbons are colored cyan). Oxygens are colored red, nitrogens blue, and sulfurs yellow. Hydrogen bonds are indicated with dashed lines.

In contrast, 1,3-dimethylpyrazole substitution (**13**) was found to be detrimental to JAK2 potency and selectivity, probably due to lack of the hydrogen bonding interaction with Tyr931 and suboptimal hydrophobic interaction with the extended hinge region. Consistent with our model, removal of the methyl group from the pyrazole nitrogen (**14**) led to significant loss of JAK family selectivity.

Although compound **12** displayed superior JAK family selectivity, it demonstrated higher potential for QT prolongation in the patch clamp hERG channel assay (75% and 20% inhibition for **12** and BMS-911543 at 30  $\mu\text{M}$ , respectively). In addition, **12** also showed an inferior pharmacokinetic profile compared to BMS-911543 and hence was not progressed further for additional studies.

BMS-911543 and related pyrazoles were synthesized using the reaction sequence depicted in Scheme 3. Condensation of **2**

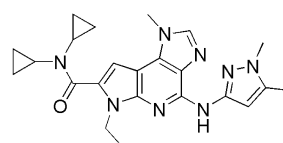
Scheme 3<sup>a</sup>

<sup>a</sup>Reagents and conditions: (a) NaH, 4,4-bis(methylthio)but-3-en-2-one, DMF, RT, 75%; (b) methyl hydrazine, EtOH, 85 °C, 30%; (c) *tert*-butyl 1-methylhydrazinecarboxylate, AcOH, 50 °C; (d) formic acid, 60 °C, 65%.

with 4,4-bis(methylthio)but-3-en-2-one gave intermediate **15**. Initially, **14** was directly combined with methyl hydrazine furnishing a 1:9 mixture of desired 1,5- and undesired 1,3-dimethylpyrazole regioisomers (BMS-911543 and **13**, respectively).<sup>20</sup> By subjecting **15** to condensation with *tert*-butyl 1-methylhydrazinecarboxylate followed by subsequent treatment with formic acid, BMS-911543 was formed exclusively.<sup>21</sup> The reaction sequence proceeds through the kinetically formed intermediate **16**, which undergoes cyclization after Boc-deprotection to yield the desired regioisomer. Pyrazoles **12** and **14** were prepared from **15** in analogous manner as BMS-911543.

In cellular assays, BMS-911543 showed potent antiproliferative activity in the SET-2 as well as BaF3-V617F engineered cell lines (both dependent upon JAK2 pathway), with IC<sub>50</sub> values of 60 and 70 nM, respectively. The antiproliferative activity of BMS-911543 in SET-2 and BaF3-V617F cells correlated with similar activity on constitutively active pSTAT5 (IC<sub>50</sub> 80 and 65 nM, respectively). In contrast, non-JAK2-

dependent cell lines (A549, MDA-MB-231, MiaPaCa-2) were significantly less sensitive to the inhibitor treatment. The excellent biochemical selectivity versus JAK1/3 translated to good cellular and functional selectivity in an IL-2 mediated T-cell proliferation assay (IC<sub>50</sub> 990 nM).<sup>12</sup> Also, cell lines that rely on other JAK family members, including CTLL2 and parental BaF3 cells stimulated with IL-3, showed weak antiproliferative activity for BMS-911543 (IC<sub>50</sub> 2.9 and 3.5  $\mu\text{M}$ , respectively) (Figure 5).<sup>12</sup>

**JAK Family Selectivity:**

JAK2 IC<sub>50</sub> = 1.1 nM (K<sub>i</sub> = 0.48 nM)  
 JAK3 IC<sub>50</sub> = 75 nM (K<sub>i</sub> = 360 nM)  
 JAK1 IC<sub>50</sub> = 360 nM (K<sub>i</sub> = 110 nM)  
 TYK2 IC<sub>50</sub> = 66 nM

**Cellular and Functional Activity:**

Cellular:  
 SET2 IC<sub>50</sub> = 60 nM  
 BaF3-V617F IC<sub>50</sub> = 61 nM  
 A549 IC<sub>50</sub> = 2400 nM  
 Ba/F3 + IL-3 IC<sub>50</sub> = 3500 nM  
 CTLL2 IC<sub>50</sub> = 2900 nM

Functional:  
 IL-2 mediated T Cell Prol IC<sub>50</sub> = 990 nM  
 (JAK1/3)

**Mechanistic:**

SET2 pSTAT5 IC<sub>50</sub> = 80 nM  
 BaF3-V617F pSTAT5 IC<sub>50</sub> = 70 nM

Figure 5. Biochemical and cellular data summary of BMS-911543.

BMS-911543 suppressed the pSTAT5 levels (mediated by wild type JAK2) relative to vehicle control when stimulated with thrombopoietin (TPO) in a mouse pharmacodynamic model.<sup>12</sup> The responses were dose dependent and resulted in nearly complete normalization of pSTAT5 levels for 18 h at the highest oral dose of 30 mg/kg. At an intermediate 10 mg/kg oral dose, ~65% reduction was observed up to 18 h, whereas at the 5 mg/kg dose, approximately 50% reduction in pSTAT5 for 8 h was achieved. Observed pSTAT5 reductions correlated with exposures of BMS-911543, with AUC<sub>0-8h</sub> values of 23, 41, and 109  $\mu\text{M}\cdot\text{h}$ , respectively, for dose levels of 5, 10, and 30 mg/kg. In addition, BMS-911543 demonstrated a potent and sustained (2 mg/kg up to 7 h) PD effect in blocking pSTAT5 formation in mice grafted with human SET-2 cells harboring JAK2-V617F mutation.

In *in vitro* ADMET profiling assays, BMS-911543 showed good metabolic stability, excellent intrinsic permeability, and moderate drug–drug interaction potential based upon CYP inhibition of the CYP3A4 and CYP1A2 isoforms. In an *in vitro* safety panel consisting of 45 targets, BMS-911543 showed IC<sub>50</sub> > 25  $\mu\text{M}$  for all targets except PDE4 (IC<sub>50</sub> 5.6  $\mu\text{M}$ ). BMS-911543 was not mutagenic or clastogenic in exploratory Ames and *in vitro* micronucleus assays, respectively. In addition to weak activity in the patch clamp hERG assay, BMS-911543 also showed similar trends in *in vitro* Na<sup>+</sup> and Ca<sup>2+</sup> binding assays, indicating a low potential to cause cardiovascular effects (Table 3). In *in vitro* biotransformation studies with human liver microsomes, BMS-911543 formed small amounts (~4%) of 1-demethylated metabolite (compound **14**) as the major metabolite.

The pharmacokinetics of BMS-911543 was investigated in mice, rats, dogs, and monkeys (Table 4 and Supporting Information). The absolute oral bioavailability in solution was



**Table 3. In Vitro ADMET Profile of BMS-911543**

metabolic stability ( $T_{1/2}$ min)	49 (H), 108 (M), 69 (R), 70 (D)
PAMPA (pH 7.4)	698 nm/sec
HLM CYP $IC_{50}$	all >40 $\mu$ M; except CYP3A4 (3 $\mu$ M) and 1A2 (1 $\mu$ M)
hERG patch clamp	20% inh at 30 $\mu$ M
Na <sup>+</sup> patch clamp	<10% inh at 10 $\mu$ M (1 Hz and 4 Hz)
Ca <sup>2+</sup> patch clamp $IC_{50}$	>80 $\mu$ M
PXR $EC_{50}$	>50 $\mu$ M
HEPG2 $IC_{50}$	>50 $\mu$ M

**Table 4. Pharmacokinetic Profile of BMS-911543**

PK	mouse <sup>a</sup>	rat <sup>b</sup>	dog <sup>c</sup>	cyno <sup>d</sup>
CL (mL/min/kg)	0.55	0.7	6.5	5.3
V <sub>ss</sub> (L/kg)	0.26	0.3	1.6	1.1
$T_{1/2}$ (h)	5.1	5	2.2	2.4
F (%)	100	100	82	53

<sup>a</sup>Mice were dosed 2.0 mg/kg IV and 10.0 mg/kg PO. <sup>b</sup>Rats were dosed 1.0 mg/kg IV and 1.0 mg/kg PO. <sup>c</sup>Dogs were dosed 0.2 mg/kg IV and 0.2 mg/kg PO. <sup>d</sup>Cyno were dosed 1.0 mg/kg IV and 1.0 mg/kg PO.

>50% in all the species tested. In addition, the absorption of BMS-911543 was not significantly impacted by particle dissolution (suspension formulation), with a relative bioavailability (vs solution) of ~60% in rats and ~100% in dogs.

In single-dose toxicological studies, BMS-911543 was well tolerated up to 100 mg/kg in rats (mean  $AUC_{0-72h}$  11300  $\mu$ M·h) and dogs ( $AUC_{0-24}$  610  $\mu$ M·h). In two-week repeat dose studies in rats, a 15 mg/kg/day dose (Day 14  $AUC_{0-24}$  3200  $\mu$ M·h) was well tolerated. The most sensitive effects observed were decreases in reticulocytes and subsequent reductions in red blood cell mass. These effects, and observed decreases in platelets, are consistent with JAK2 inhibition.

In summary, ADMET and X-ray structure-guided refinement of the C-4 heterocycle to address metabolic liability present in 4,5-dimethylthiazole **1** led to the discovery of BMS-911543 (**11**), with excellent kinome selectivity, *in vivo* pharmacodynamic activity, and safety profile. BMS-911543 is currently in clinical trials for the treatment of MF.<sup>22</sup>

## ■ ASSOCIATED CONTENT

### Ⓢ Supporting Information

Full experimental details for key compounds and biological protocols. The Supporting Information is available free of charge on the ACS Publications website at DOI: 10.1021/acsmchemlett.5b00226.

## ■ AUTHOR INFORMATION

### Corresponding Author

\*Tel: +1-609-252-4320. E-mail: ashok.purandare@bms.com.

### Present Addresses

<sup>†</sup>Immunomedics, 300 The American Road, Morris Plains, New Jersey 07950, United States.

<sup>‡</sup>Xenex, 121 Interpark, Suite 104, San Antonio, Texas 78216, United States.

<sup>§</sup>Janssen Pharmaceutical Companies of Johnson and Johnson, 1400 McKean Rdo, Spring House, Pennsylvania 19002, United States.

<sup>||</sup>BioMotiv, 20600 Chagrin Boulevard, Suite 210, Cleveland, Ohio 44122, United States.

<sup>‡</sup>ARMGO Pharma Inc., 777 Old Saw Mill River Road, Tarrytown, New York 10591, United States.

<sup>#</sup>Biocon BMS R&D Center (BBRC), Bangalore, Syngene International Ltd., Plot No. 2 and 3, Bommasandra IV Phase, Jigani Link Road, Bangalore 560 099, India.

### Author Contributions

All authors have given approval to the final version of the manuscript.

### Notes

The authors declare no competing financial interest.

## ■ ACKNOWLEDGMENTS

We thank Drug Discovery, Synthesis, Rulin Zhao and Bei Wang for their help in preparation of BMS-911543. We also thank T. G. Murali Dhar for his critical input during the preparation of the manuscript.

## ■ REFERENCES

- (1) Campbell, P.; Green, A. The Myeloproliferative Disorders. *N. Engl. J. Med.* **2006**, *355*, 2452–66.
- (2) Morgan, K.; Gilliland, G. A Role for JAK2 Mutations in Myeloproliferative Diseases. *Annu. Rev. Med.* **2008**, *59*, 213–22 and references cited therein.
- (3) Anand, S.; Huntly, B. Disordered Signaling in Myeloproliferative Neoplasms. *Hematol. Oncol. Clin. N. Am.* **2012**, *26*, 1017–1035.
- (4) Tefferi, A. Essential thrombocythemia, polycythemia vera, and myelofibrosis: current management and the prospect of targeted therapy. *Am. J. Hematol.* **2008**, *83*, 491–497.
- (5) Wernig, G.; Mercher, T.; Okabe, R.; Levine, R.; Lee, B.; Gilliland, D. G. Expression of JAK2V617F causes a polycythemia vera-like disease with associated myelofibrosis in a murine bone marrow transplant model. *Blood* **2006**, *107*, 4274–4281.
- (6) Pardanani, A.; Hood, J.; Lasho, T.; Levine, R.; Martin, M.; Noronha, G.; Finke, C.; Mak, C.; Mesa, R.; Zhu, H.; Soll, R.; Gilliland, G.; Tefferi, A. TG101209, a small molecule JAK2-selective kinase inhibitor potently inhibits myeloproliferative disorder-associated JAK2V617F and MPLW515L/K mutations. *Leukemia* **2007**, *21*, 1658–1668.
- (7) Cervantes, F.; Vannucchi, A.; Kiladjan, J.; Al-Ali, H.; Sirulnik, A.; Stalbovskaya, V.; McQuitty, M.; Hunter, D.; Levy, R.; Passamonti, F.; Barbui, T.; Barosi, G.; Harrison, C.; Knoops, L.; Gisslinger, H. Three-year efficacy, safety, and survival findings from COMFORT-II, a phase 3 study comparing ruxolitinib with best available therapy for myelofibrosis. *Blood* **2013**, *122*, 4047–53.
- (8) Pardanani, A.; Gotlib, J.; Jamieson, C.; Cortes, J.; Talpaz, M.; Stone, R.; Silverman, M.; Gilliland, G.; Shorr, J.; Tefferi, A. Safety and Efficacy of TG101348, a Selective JAK2 Inhibitor, in Myelofibrosis. *J. Clin. Oncol.* **2011**, *29*, 789–96.
- (9) William, A. D.; Lee, A. C.; Blanchard, S.; Poulsen, A.; Teo, E. L.; Nagaraj, H.; Tan, E.; Chen, D.; Williams, M.; Sun, E. T.; Goh, K. C.; Ong, W. C.; Goh, S. K.; Hart, S.; Jayaraman, R.; Pasha, M. K.; Ethirajulu, K.; Wood, J. M.; Dymock, B. W. Discovery of the Macrocyclic 11-(2-Pyrrolidin-1-yl-ethoxy)-14,19-dioxo-5,7,26-triazatetracyclo[19.3.1.1(2,6).1(8,12)]heptacosal(25,2(26),3,5,8,10,12(27),16,21,23-decaene (SB1518), a Potent Janus Kinase 2/Fms-Like Tyrosine Kinase-3 (JAK2/FLT3) Inhibitor for the Treatment of Myelofibrosis and Lymphoma. *J. Med. Chem.* **2011**, *54*, 4638–58.
- (10) Tam, C.; Verstovsek, S. Investigational Janus kinase inhibitors. *Expert Opin. Invest. Drugs* **2013**, *22*, 687–699.
- (11) Hart, A. C.; Schroeder, G. M.; Wan, H.; Inghrim, J.; Grebinski, J.; Kempson, J.; Guo, J.; Pitts, W. J.; Tokarski, J. S.; Sack, J. S.; Khan, J. A.; Lippy, J.; Lorenzi, M. V.; You, D.; McDevitt, T.; Vuppugalla, R.; Zhang, Y.; Lombardo, L. J.; Trainor, G. L.; Purandare, A. V. Structure-based design of selective Janus kinase 2 pyrrolopyridine inhibitors. Manuscript submitted. *ACS Med. Chem. Lett.* **2015**, DOI: 10.1021/acsmchemlett.5b00225.

(12) Purandare, A. V.; McDevitt, T. M.; Wan, H.; You, D.; Penhallow, B.; Han, X.; Vuppugalla, R.; Zhang, Y.; Ruepp, S. U.; Trainor, G. L.; Lombardo, L.; Pedicord, D.; Gottardis, M. M.; Ross-Macdonald, P.; de Silva, H.; Hosbach, J.; Emanuel, S. L.; Blat, Y.; Fitzpatrick, E.; Taylor, T. L.; McIntyre, K. W.; Michaud, E.; Mulligan, C.; Lee, F. Y.; Woolfson, A.; Lasho, T. L.; Pardanani, A.; Tefferi, A.; Lorenzi, M. V. Characterization of BMS-911543, a functionally selective small-molecule inhibitor of JAK2. *Leukemia* **2012**, *26*, 280–288.

(13) Obach, S.; Kalgutkar, A.; Ryder, T.; Walker, G. In Vitro Metabolism and Covalent Binding of Enol-Carboxamide Derivatives and Anti-Inflammatory Agents Sudoxicam and Meloxicam: Insights into the Hepatotoxicity of Sudoxicam. *Chem. Res. Toxicol.* **2008**, *21*, 1890–1899.

(14) Thompson, T. N. Optimization of Metabolic Stability as a Goal of Modern Drug Design. *Med. Res. Rev.* **2001**, *21*, 412.

(15) Purandare, A. V.; Grebinski, J. W.; Hart, A.; Inghrim, J.; Schroeder, G.; Wan, H. Preparation of dicyclopropylidimidazopyrrolopyridinecarboxamide derivatives for use as JAK2 inhibitors (Bristol-Myers Squibb). PCT Int. Appl. WO2011028864, 2011.

(16) Das, J.; Furch, J.; Liu, C.; Moquin, R.; Lin, J.; Spergel, S.; McIntyre, K.; Shuster, D.; O'Day, K.; Penhallow, B.; Hung, C.; Dowejko, A.; Kamath, A.; Zhang, H.; Marathe, P.; Kanner, S.; Lin, T.; Dodd, J.; Barrish, J.; Wityak, J. Discovery and SAR of 2-amino-5-(thioaryl)thiazoles as potent and selective Itk inhibitors. *Bioorg. Med. Chem. Lett.* **2006**, *16*, 3706.

(17) Dhar, T. G. M.; Liu, C.; Pitts, W. J.; Guo, J.; Watterson, S. H.; Gu, H.; Fleener, C. A.; Katherine Sherbina, N. Z. R.; Barrish, J. C.; Hollenbaugh, D.; Iwanowicz, E. J. *Bioorg. Med. Chem. Lett.* **2002**, *12*, 3125.

(18) Fabian, M. A.; Biggs, W. H.; Treiber, D. K.; Atteridge, C. E.; Azimioara, M. D.; Benedetti, M. G.; Carter, T. A.; Ciceri, P.; Edeen, P. T.; Floyd, M.; Ford, J. M.; Galvin, M.; Gerlach, J. L.; Grotzfeld, R. M.; Herrgard, S.; Insko, D. E.; Insko, M. A.; Lai, A. G.; Lélias, J. M.; Mehta, S. A.; Milanov, Z. V.; Velasco, A. M.; Wodicka, L. M.; Patel, H. K.; Zarrinkar, P. P.; Lockhart, D. J. A small molecule-kinase interaction map for clinical kinase inhibitors. *Nat. Biotechnol.* **2005**, *23*, 329.

(19) The atomic coordinates of BMS-911543 have been deposited in the RCSB Protein Data Bank (code SCF8).

(20) Mahata, P. K.; Kumar, S.; Sriram, V.; Ila, H.; Junjappa, H. 1-Bis(methoxy)-4-bis(methylthio)-3-buten-2-one: useful three carbon synthon for synthesis of five and six membered heterocycles with masked (or unmasked) aldehyde functionality. *Tetrahedron* **2003**, *59*, 2631–2639.

(21) Park, O.; Kim, J.; Koh, M.; Park, B. Efficient Parallel Synthesis of Privileged Benzopyranylpyrazoles via Regioselective Condensation of  $\beta$ -Keto Aldehydes with Hydrazines. *J. Comb. Chem.* **2009**, *11*, 315–326.

(22) Multiple Ascending Dose of BMS-911543. <https://clinicaltrials.gov/ct2/show/NCT01236352>.